Elucidating the nicotinic acid degradation pathway in *Bacillus niacini*: Investigating the catabolic function of a flavin monooxygenase (FMO), domain of unknown function (DUF), and hypothetical protein (HP)

Abigail A. Lyon, and Mark J. Snider; Program in Biochemistry and Molecular Biology, The College of Wooster, Ohio

Background and Significance

- In our environment, things such as pharmaceuticals, pesticides, and fossil fuel use leach pollution into our soil and groundwater by releasing organic molecules called *N*-HACs or *N*-heterocyclic aromatic compounds.

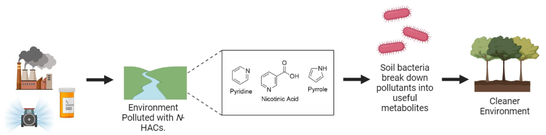

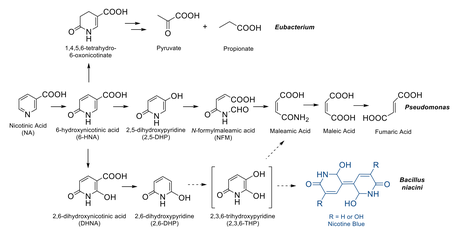

Scheme 1. Nicotinic acid degradation pathways in three bacterial species. The degradation pathways of *Eubacteriumm* (top) and *Pseudomonas* (middle) are more defined compared to that within *Bacillus* (bottom). Specifically, the pathway intermediates formed following DHNA in the *B. niacini* NA degradation pathway are under current investigation. Solid arrows show steps that have been observed experimentally while dashed lines represent hypothesized steps.

Understanding of the *B. niacini* pathway

Figure 1. *B. niacini* NA operon determined by RNA sequencing. The metabolic operon that is used for nicotinic acid degradation in *B. niacini.* Displays the enzymes used in the *B. niacini* NA degradation pathway and other proteins such as transcription regulators and chaperone proteins. Figure from Helton (1).

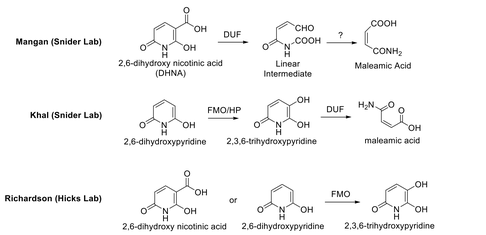

Scheme 2. Evolution of conclusions in the characterization of the FMO, DUF, and HP enzymes.

Table 1. Integration values of elutes from reaction assays containing combinations of FMO, DUF, and HP. Integration values are in millions of count. Reaction mixtures were incubated at 25°C for 30 minutes without DHP and 30 minutes with. Integration values of elutes were collected after 3 hours. The λ_{max} values used to collected integration values for each compound are shown in the second column. All samples contain NADH and DHP.

Compound	Wavelength	DHP + NADH	FMO	FMO + HP	FMO + DUF	FMO + DUF + HP
NAD^+	260 nm	0.31	0.73	0.76	2.6	2.5
DHP	320 nm	4.6	4.0	3.7	2.0	2.2
NADH	340 nm	0.93	0.67	0.59	0.08	0.1
Nicotine Blue	600 nm	1.0	1.2	1.2	1.7	1.8

Research Question & Objectives

What biochemical roles do FMO, DUF, and HP hold in the NA degradation pathway of *B. niacini*?

- Use SEC to investigate a possible complex between DUF and FMO.
- Use AlphaFold to generate predicted 3D structures of DUF and HP.
- Use Q-TOF to view possible downstream products with combinations of FMO, DUF, and HP.

Prediction of DUF structure and comparison to other protein structures in the PDB

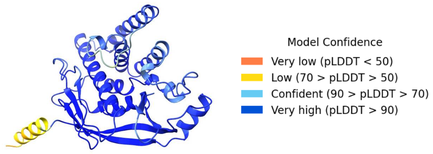

Figure 2. Predicted 3D structure of the *B. niacini* DUF enzyme. Structure was generated using AlphaFold Deepmind's Colab notebook (2, 3). pLDDT is a confidence score used to determine how confident AlphaFold is in its prediction based on residue distances.

Table 2. Highest structural matches to the predicted DUF structure. A Z-score demonstrates similarities between the query structure and structures in the DALI database (4). RMSD (root-mean-square deviation) gives the average deviation in distance between the aligned Cα atoms of two proteins.

Z-Score	RMSD	NRES	% ID	PDB ID	Name
6.1	3.1	180	18	4N6W	PREDICTED HD PHOSPHOHYDROLASE PHNZ
6.3	3.3	482	14	6PC1	GUANOSINE PENTAPHOSPHATE PHOSPHOHYDROLASE
5.4	3.8	363	18	4ME4	METAL DEPENDENT PHOSPHOHYDROLASE
5.2	7.2	479	16	4QG4	DEOXYNUCLEOSIDE TRIPHOSPHATE TRIPHOSPHOHYDROLASE
3.9	3.8	258	16	2HUO	MOLECULE: INOSITOL OXYGENASE

No evidence of an FMO/DUF complex and oligomeric status of FMO and DUF

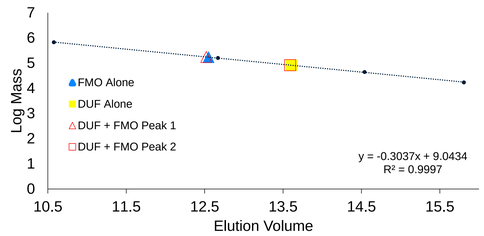

Figure 4. Calibration curve used to determine molecular weight of FMO and DUF. The curve was generated using 4 proteins of known molecular weight (Thyroglobulin, y-Globulin, Ovalbumin, Myoglobulin).

Table 4. Resulting masses from SEC to determine multimer status of DUF and possibility of an FMO/DUF complex.

Enzyme(s)	Elution Volume	Log Mass From Graph	Calculated Mass (kDa)	Expected Monomeric Mass	Oligomeric Status
DUF Alone	13.61	4.91	81.3	33	Trimer
FMO Alone	12.55	5.23	171	50	Trimer
DUF + FMO Peak 1	12.52	5.24	174	33+50	Separate Trimers
DUF + FMO Peak 2	13.59	4.92	82.4	33+50	Separate Trimers

Prediction of HP structure and comparison to other protein structures in the PDB

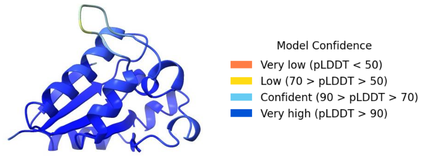

Figure 3. Predicted 3D structure of the *B. niacini* HP enzyme. Structure was generated using AlphaFold Deepmind's Colab notebook (2, 3). pLDDT is a confidence score used to determine how confident AlphaFold is in its prediction based on residue distances.

Table 3. Highest structural matches to the predicted HP structure. A Z-score demonstrates similarities between the query structure and structures in the DALI database (4). RMSD (root-mean-square deviation) gives the average deviation in distance between the aligned Cα atoms of two proteins.

Z-Score	RMSD	NRES	% ID	PDB ID	Name
18.1	2.0	121	22	3MCM	DSRE/DSRF-LIKE FAMILY PROTEIN
16.7	1.9	160	19	3PNX	PUTATIVE SULFURTRANSFERASE DSRE
16.6	1.7	117	19	1JX7	HYPOTHETICAL PROTEIN YCHN
14.4	2.1	130	20	2D1P	HYPOTHETICAL UPF0163 PROTEIN YHEN

THP may spontaneously and rapidly ring-open to form a carbamic acid intermediate

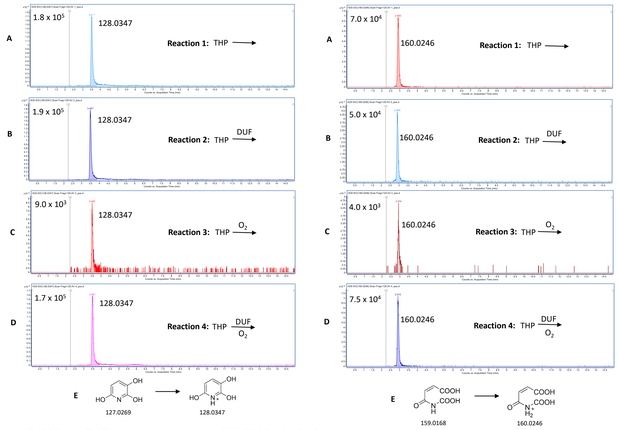

Figure 5. EICs of THP scanning for m/z = 128.0347. (A) THP in anaerobic buffer. **(B)** THP incubated with DUF in anaerobic buffer. **(C)** THP in aerobic buffer. **(D)** THP incubated with DUF in aerobic buffer. **(E)** Structure of THP and the corresponding exact masses of it and of its $[M+H]^+$ ion.

Figure 6. EICs of carbamic acid intermediate scanning for m/z = 160.0246. (A) THP in anaerobic buffer. **(B)** THP incubated with DUF in anaerobic buffer. **(C)** THP in aerobic buffer. **(D)** THP incubated with DUF in aerobic buffer. **(E)** Structure of the carbamic acid intermediate and the corresponding exact masses of it and of its $[M+H]^+$ ion.

Possible relation to the NA degradation pathway of *A. nidulans* (fungus)

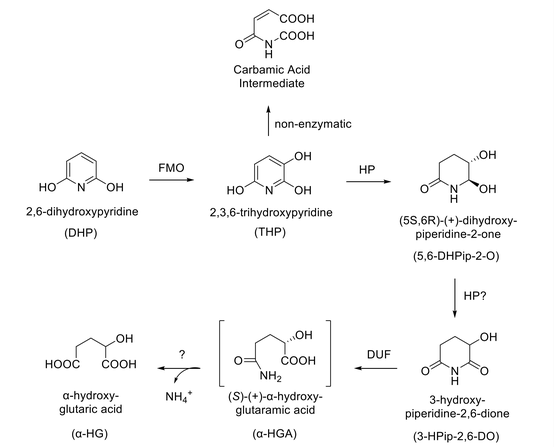

Scheme 3. Hypothesized pathway from THP for the degradation of nicotinic acid in *B. niacini*. The evidence of a reduced THP intermediate suggests that HP may reduce and then possibly oxidize THP after its formation via FMO. DUF would then catalyze the ring opening of the 3-HPip-2,6-DO intermediate. This pathway is modeled after the degradation of nicotinic acid in *A. nidulans*, a eukaryotic fungus (5).

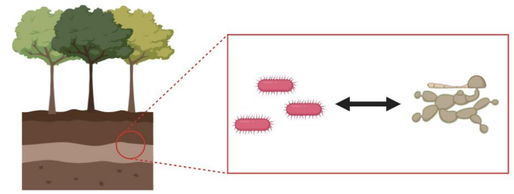

Future Research

1. Analyze fragmentation patterns of the ion at 130.0504.
2. Further bioinformatic analysis of the various enzymes looking at possible complexes.
3. Identify the cofactor (if one is needed) DUF utilizes to be an active enzyme.

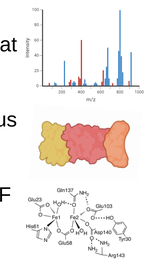

FMO and HP together catalyze the hydroxylation and ring reduction of 2,6-DHP: Evidence for new intermediates in the *B. niacini* nicotinate degradation pathway

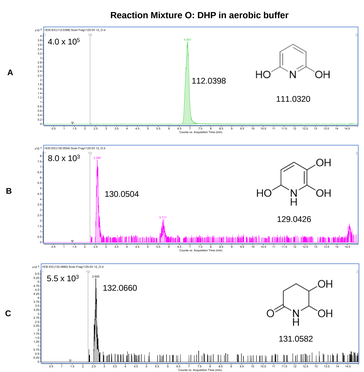

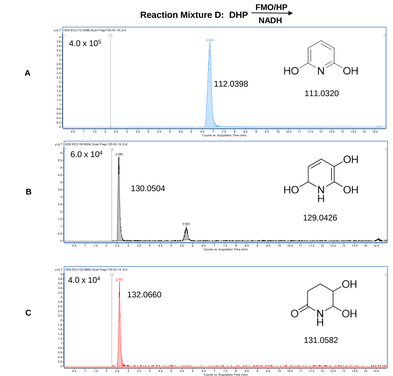

Figure 7. DHP in aerobic buffer contains reduced forms of THP. EICs of DHP in aerobic buffer (reaction mixture O). **(A)** EIC for DHP. **(B)** EIC for partially reduced THP. **(C)** EIC for fully reduced THP labeled 5,6-DHPip-2O.

Figure 8. DHP with FMO and HP in aerobic buffer shows an increase in reduced forms of THP compared to DHP in aerobic buffer. (A) EIC for DHP. **(B)** EIC for partially reduced THP. **(C)** EIC for fully reduced THP labeled 5,6-DHPip-2O.

Table 5. Increased peak height corresponding to a partially reduced THP molecule and a fully reduced THP molecule (5,6-DHPip-2O). Peak heights were determined from EICs from the TIC based on the $[M+H]^+$ ion for each molecule.

Reaction Assay	Peak Height for DHP	Peak Height for Reduced THP	Peak Height for Reduced THP (5,6-DHPip-2O)
Sample O: DHP in aerobic buffer with no *Bn* enzymes	4.0×10^5	8.0×10^3	5.5×10^3
Sample D: DHP + FMO + HP + NADH	4.0×10^5	6.0×10^4	4.0×10^4
% Change	0%	650% increase	627% increase

Acknowledgements

- Whitmore-Williams Science Scholarship
- NSF Grant #1817535
- College of Wooster Senior Independent Study

References

1. Helton, N. (2020) Progress in Characterizing a Novel Root Exudate: Differential gene expression of Bacillus niacini DSM 2993 in Response to Nicotinic Acid through RNA-seq. *Independent study thesis at the College of Wooster*
2. Jumper, J., Evans, R., Pritzel, A., Green, T., Figurnov, M., Ronneberger, O., Tunyasuvunakool, K., Bates, R., Žídek, A., Potapenko, A., Bridgland, A., Meyer, C., Kohl, S. A. A., Ballard, A. J., Cowie, A., Romera-Paredes, B., Nikolov, S., Jain, R., Adler, J., Back, T., Petersen, S., Reiman, D., Clancy, E., Zielinski, M., Steinegger, M., Pacholska, M., Berghammer, T., Bodenstein, S., Silver, D., Vinyals, O., Senior, A. W., Kavukcuoglu, K., Kohli, P., and Hassabis, D. (2021) Highly accurate protein structure prediction with AlphaFold. *Nature*. **596**. 583–589
3, Varadi, M., Anyango, S., Deshpande, M., Nair, S., Natassia, C., Yordanova, G., Yuan, D., Stroe, O., Wood, G., Laydon, A., Žídek, A., Green, T., Tunyasuvunakool, K., Petersen, S., Jumper, J., Clancy, E., Green, R., Vora, A., Lutfi, M., Figurnov, M., Cowie, A., Hobbs, N., Kohli, P., Kleywegt, G., Birney, E., Hassabis, D., and Velankar, S. (2022) AlphaFold Protein Structure Database: massively expanding the structural coverage of protein-sequence space with high-accuracy models. *Nucleic Acids Research*, **50**, D439–D444
4, DALI shines a light on remote homologs: One hundred discoveries - Holm - 2023 - Protein Science - Wiley Online Library [online]
5. Bokor, E., Ámon, J., Varga, M., Szekeres, A., Hegedüs, Z., Jakusch, T., Szakonyi, Z., Flipphi, M., Vágvölgyi, C., Gácser, A., Scazzocchio, C., and Hamari, Z. (2022) A complete nicotinate degradation pathway in the microbial eukaryote Aspergillus nidulans. *Commun Biol.* **5**, 1–11